J. Fluid Mech. (1985), *vol.* 152, *pp.* 113–123
Printed in Great Britain

Nonlinear thermal convection with finite conducting boundaries

By N. RIAHI
Department of Theoretical and Applied Mechanics, University of Illinois at Urbana–Champaign, Urbana, Illinois 61801

(Received 3 October 1983 and in revised form 23 April 1984)

Finite-amplitude thermal convection in a horizontal layer with finite conducting boundaries is investigated. The nonlinear steady problem is solved by a perturbation technique, and the preferred mode of convection is determined by a stability analysis. Square cells are found to be the preferred form of convection in a semi-infinite three-dimensional region Ω in the (γ_b, γ_t, P)-space (γ_b and γ_t are the ratios of the thermal conductivities of the lower and upper boundaries to that of the fluid and P is the Prandtl number). Two-dimensional rolls are found to be the preferred convection pattern outside Ω. The dependence on γ_b, γ_t and P of the heat transported by convection is computed for the various solutions analysed in the paper.

1. Introduction

In a recent study of the problem of finite-amplitude thermal convection in a porous layer with infinite Prandtl–Darcy number and finite conducting boundaries (Riahi 1983, henceforth referred to as R83) it was shown, in particular, that square-flow pattern convection is preferred in a bounded region Γ in the (γ_b, γ_t)-space (where γ_b and γ_t are the ratios of the thermal conductivities of the lower and upper boundaries to that of the fluid) and that two-dimensional rolls are the preferred flow pattern outside Γ. The same method of analysis is applied in the present study to steady nonlinear Rayleigh–Bénard convection and its stability in the case of finite conducting boundaries and arbitrary Prandtl numbers P. An important result of the present study is that square cells are the preferred form of convection in a semi-infinite three-dimensional region Ω in the (γ_b, γ_t, P)-space, while two-dimensional rolls are the preferred convection pattern outside Ω.

An analysis similar to the present one has been performed recently by Jenkins & Proctor (1984, henceforth referred to as JP) to study the case of symmetric boundary conditions for convection at the transition boundary between rolls and squares. The present paper studies both cases of symmetric and asymmetric boundary conditions for complete domain of convection at arbitrary values of γ_b and γ_t, and the subsequent results demonstrate that there can exist significant qualitative differences between the results of these two cases. Discussion of the results of the present study and a comparison with those in JP are given in some detail in §3.

2. Analysis and results

We consider an infinite horizontal fluid layer of depth d heated from below and bounded above and below by two rigid half-spaces with thermal conductivities λ_t^e and λ_b^e respectively. In the steady static state a constant heat flux traverses the system such that the temperatures T_1 and T_2 are attained at the upper and lower boundaries of the fluid. Under the usual Boussinesq approximation, the non-dimensional forms of the equations for momentum, heat and conservation of mass can be simplified by using the general representation

$$\boldsymbol{u} = \boldsymbol{\delta}\phi + \boldsymbol{\epsilon}\psi, \tag{1a}$$

$$\boldsymbol{\delta} \equiv \nabla \times \nabla \times (\boldsymbol{z}\ \ ), \quad \boldsymbol{\epsilon} \equiv \nabla \times (\boldsymbol{z}\ \ ), \tag{1b}$$

for the divergent free velocity vector field $\boldsymbol{u}$. Here $\boldsymbol{z}$ represent a unit vector in the vertical direction. The detailed analysis (Schluter, Lortz & Busse 1965) indicates that the terms containing ψ in the governing equations are insignificant since the toroidal component $\boldsymbol{\epsilon}\psi$ of $\boldsymbol{u}$ is of the order of the mth ($m \geqslant 3$) power of amplitude ϵ of convection, and thus cannot enter the analysis discussed here. Therefore we simply set $\psi = 0$ in (1). Taking the vertical component of the double curl of the momentum equation and using (1) in the heat equation yields the following governing equations:

$$\Delta_2\left(\nabla^4\phi - \theta - \frac{\partial}{\partial t}\nabla^2\phi\right) = P^{-1}\boldsymbol{\delta}\cdot[\boldsymbol{\delta}\phi\cdot\nabla(\boldsymbol{\delta}\phi)], \tag{2a}$$

$$\left(\nabla^2 - \frac{\partial}{\partial t}\right)\theta - R\Delta_2\phi = \boldsymbol{\delta}\phi\cdot\nabla\theta, \tag{2b}$$

where θ is the deviation of the temperature from its static value,

$$R = \beta(T_2 - T_1)\,gd^3\rho_0\,c/\nu\lambda$$

is the Rayleigh number, ρ_0 is the reference density, c is the specific heat at constant pressures, β is the coefficient of thermal expansion, ν is the kinematic viscosity, g is the acceleration due to gravity, $P = \nu\rho_0\,c/\lambda$ is the Prandtl number, λ is the thermal conductivity of the fluid, and Δ_2 is the horizontal Laplacian.

Introducing a Cartesian system of coordinates, with the origin on the midplane of the layer and with the z-coordinate in the vertical direction, the boundary conditions for θ and ϕ can be written as

$$\phi = \frac{\partial\phi}{\partial z} = 0 \quad \text{at } z = \pm\tfrac{1}{2}, \tag{3a}$$

$$\frac{\partial\theta}{\partial z} = \gamma_{\mathrm{b}}\frac{\partial\theta_{\mathrm{b}}^{\mathrm{e}}}{\partial z}, \quad \theta = \theta_{\mathrm{b}}^{\mathrm{e}} \quad \text{at } z = -\tfrac{1}{2}, \tag{3b}$$

$$\frac{\partial\theta}{\partial z} = \gamma_{\mathrm{t}}\frac{\partial\theta_{\mathrm{t}}^{\mathrm{e}}}{\partial z}, \quad \theta = \theta_{\mathrm{t}}^{\mathrm{e}} \quad \text{at } z = \tfrac{1}{2}, \tag{3c}$$

where $\gamma_{\mathrm{b}} = \lambda_{\mathrm{b}}^{\mathrm{e}}/\lambda$, $\gamma_{\mathrm{t}} = \lambda_{\mathrm{t}}^{\mathrm{e}}/\lambda$, and $\theta_{\mathrm{b}}^{\mathrm{e}}$ and $\theta_{\mathrm{t}}^{\mathrm{e}}$ describe the deviations from the static temperature distribution in the spaces $z \leqslant -\tfrac{1}{2}$ and $z \geqslant \tfrac{1}{2}$ respectively.

The linear planeform function $w(x, y)$ has the representation

$$w(x,y) = \sum_{n=-N}^{N} c_n w_n \equiv \sum_{n=-N}^{N} c_n \exp(\mathrm{i}\boldsymbol{K}_n\cdot\boldsymbol{r}), \tag{4}$$

and satisfies the relation

$$\Delta_2 w = -\alpha^2 w, \quad \langle ww\rangle = 1. \tag{5}$$

Here α is the horizontal wavenumber, angular brackets indicate an average over the fluid layer, $\boldsymbol{r}$ is the position vector, and the horizontal wavenumber vectors $\boldsymbol{K}_n$ satisfy the properties

$$\boldsymbol{K}_n\cdot\boldsymbol{z} = 0, \quad |\boldsymbol{K}_n| = \alpha, \quad \boldsymbol{K}_{-n} = -\boldsymbol{K}_n. \tag{6}$$

	$\gamma_b = \gamma_t = \gamma$		$\gamma_b = \gamma, \gamma_t = \infty$		$\gamma_n = \gamma, \gamma_t = 0$	
γ	R_c	α_c	R_c	α_c	R_c	α_c
0	720	0	1300	2.70	720	0
0.0001	725.2	0.001	1300.1	2.70	724.1	0.001
0.001	728.1	0.20	1303.8	2.75	726.3	0.15
0.01	756.3	0.80	1315.5	2.78	746.3	0.80
0.1	873.8	1.40	1331.9	2.80	821.9	1.35
0.4	1073.8	1.85	1410.1	2.85	940	1.75
0.7	1190.2	2.35	1463.8	2.95	1010.1	2.10
1	1270.9	2.55	1497.5	2.95	1057.5	2.10
4	1533.8	2.90	1620.9	3.05	1203.8	2.45
7	1603.8	3.10	1657.5	3.10	1241.9	2.48
10	1630.2	3.10	1673.8	3.12	1257.5	2.48
100	1701.9	3.11	1707.5	3.12	1291.9	2.50
1000	1708	3.13	1708	3.13	1300.1	2.60
∞	1708	3.13	1708	3.13	1300.5	2.60

TABLE 1. Values of R_c and α_c with boundaries of different conductivity

The coefficients c_n satisfy the conditions

$$\sum_{n=-N}^{N} c_n c_n^* = 1, \quad c_n^* = c_{-n}, \tag{7}$$

where N is a positive integer and the asterisk indicates the complex conjugate.

We shall discuss the analysis of the problem, but try to avoid going into details since the main structure of the analysis and the method of solutions are essentially the same as in R83.

The steady small-amplitude convection analysis is based on the following expansions for θ, ϕ and R in powers of ϵ:

$$\left.\begin{aligned} \begin{pmatrix}\theta\\ \phi\end{pmatrix} &= \epsilon\begin{pmatrix}\theta_1\\ \phi_1\end{pmatrix} + \epsilon^2\begin{pmatrix}\theta_2\\ \phi_2\end{pmatrix} + \dots, \\ R &= R_0 + \epsilon R_1 + \epsilon^2 R_2 + \dots. \end{aligned}\right\} \tag{8}$$

When (8) is inserted into (2) and (3) and the quadratic terms are disregarded, the linear system of the problem is found (see the Appendix). Following R83 and the results given in the Appendix, the linear system leads to an equation for R_0, γ_b, γ_t and α. R_0 is a complicated implicit function of α, γ_t and γ_b through this equation, which is symmetric with respect to γ_b and γ_t. The same kind of numerical computations as those discussed in R83 are done here to determine the minimum value R_c of R_0 with respect to α attained at some $\alpha = \alpha_c$ for given γ_b and γ_t. Values of R_c and α_c for different values of γ_t and γ_b are presented in table 1. The qualitative features of these linear results are the same as those discussed in R83. The solvability condition for the equations of order ϵ^2, which are given in the Appendix, yields $R_1 = 0$ (see the Appendix). The solvability condition for the equations of order ϵ^3 (see the Appendix) yields the following set of equations:

$$\alpha_c^2 R_2 \langle \phi_1 \theta_1 \rangle c_n = \sum_{m=-N}^{N} T_{nm} c_n c_m c_m^* \quad (n = -N, \dots, -1, 1, \dots, N). \tag{9}$$

The symmetric matrix T_{nm} given in (9) has a lengthy expression, which will not be given here, and is a function of R_c, α_c, γ_b, γ_t, P and $\hat{\phi}_{mn}$, where

$$\hat{\phi}_{mn} = \alpha^{-2}(\boldsymbol{k}_m \cdot \boldsymbol{k}_n). \tag{10}$$

Equation (9), together with (7), represents an inhomogeneous system of $2N+1$ nonlinear algebraic equations for the $2N$ coefficients c_n and the coefficient R_2. The general solution of this system is not known, but a simple set of solutions can be derived in the so-called 'regular' case, in which all angles between two neighbouring $\boldsymbol{k}$-vectors are equal. The solution is simply

$$|c_i|^2 = \frac{1}{2N}, \quad i = 1, \ldots, N, \tag{11a}$$

$$2NR_2\alpha_c^2\langle\phi_1\theta_1\rangle = \sum_{m=1}^{N}(T_{1m}+T_{1,-m}). \tag{11b}$$

Using the approximate relationship

$$H = \langle\theta(\boldsymbol{z}\cdot\boldsymbol{u})\rangle \approx \epsilon^2\alpha_c^2\langle\theta_1\phi_1\rangle \approx \alpha_c^2(R-R_c)R_2^{-1}\langle\theta_1\phi_1\rangle \tag{12}$$

for the heat transported by convection, we find from (11b) and (12) the following: in the case of the two-dimensional solution in the form of rolls

$$N=1, \quad H_r = H^{\text{rolls}}(R-R_c)^{-1} = 2\alpha_c^4(\langle\phi_1\theta_1\rangle)^2(T_{11}+T_{1,-1})^{-1}; \tag{13a}$$

in the case of square-pattern convection

$$\left.\begin{aligned} N=2, \quad \hat{\phi}_{12}=0, \\ H_s = H^{\text{squares}}(R-R_c^{-1}) = 4\alpha_c^4(\langle\phi_1\theta_1\rangle)^2(T_{11}+T_{1,-1}+T_{12}+T_{1,-2})^{-1}; \end{aligned}\right\} \tag{13b}$$

and in the case of hexagonal cells

$$\left.\begin{aligned} N=3, \quad \hat{\phi}_{12}=\hat{\phi}_{23}=\hat{\phi}_{31}=\tfrac{1}{2}, \\ H_h = H^{\text{hexagons}}(R-R_c)^{-1} = 6\alpha_c^4(\langle\phi_1\theta_1\rangle)^2(T_{11}+T_{1,-1}+T_{12}+T_{1,-2}+T_{13}+T_{1,-3})^{-1}. \end{aligned}\right\} \tag{13c}$$

Since the expression for T_{nm} turns out to be a polynomial of second degree in P^{-1}, we define

$$\left.\begin{aligned} H_r &= (H_{r1}+H_{r2}P^{-1}+H_{r3}P^{-2})^{-1}, \\ H_s &= (H_{s1}+H_{s2}P^{-1}+H_{s3}P^{-2})^{-1}, \\ H_h &= (H_{h1}+H_{h2}P^{-1}+H_{h3}P^{-2})^{-1}, \end{aligned}\right\} \tag{14}$$

where the coefficients H_{ri}, H_{si} and H_{hi} ($i = 1,2,3$) are functions of α_c, R_c, γ_b and γ_t. The values of these coefficients are computed for the following three different cases: (I) both boundaries have the same conductivity γ, $\gamma_t = \gamma_b = \gamma$; (II) one of the boundaries (say the upper one) has infinite conductivity, the other has arbitrary conductivity γ, $\gamma_t = \infty$, $\gamma_b = \gamma$; (III) one of the boundaries (say the upper one) is non-conducting, the other has arbitrary conductivity γ, $\gamma_t = 0$, $\gamma_b = \gamma$. The values of H_{ri}, H_{si} and H_{hi} are presented in tables 2, 3 and 4 respectively. The results agree well with those given by Schlüter *et al.* (1965) for the case where $\gamma_b = \gamma_t = \infty$ and with those computed by Busse & Riahi (1980) for the case where $\gamma_b = \gamma_t = \gamma \ll 1$. For given values of γ and P, we have found that either $H_r > H_h$ or $H_s > H_h$. $H_s = \max(H_r, H_s, H_h)$ for all $\gamma \leqslant \gamma_1$ ($\gamma_1 \leqslant 1.5$ for case I, $\gamma_1 = 0$ for case II, and

	$\gamma_b = \gamma_t = \gamma$			$\gamma_b = \gamma, \gamma_t = \infty$			$\gamma_b = \gamma, \gamma_t = 0$		
γ	H_{r1}	H_{r2}	H_{r3}	H_{r1}	H_{r2}	H_{r3}	H_{r1}	H_{r2}	H_{r3}
0	1.143	−0.003	0.001	0.734	−0.007	0.007	1.143	−0.003	0.001
0.0001	1.143	0	0	0.734	−0.007	0.007	1.143	0	0
0.001	1.131	−0.001	0	0.724	−0.007	0.007	1.136	0	0
0.01	0.987	−0.008	0.001	0.715	−0.007	0.007	0.989	−0.008	0.001
0.1	0.787	−0.015	0.003	0.705	−0.007	0.007	0.822	−0.014	0.003
0.4	0.665	−0.016	0.006	0.680	−0.007	0.007	0.744	−0.015	0.005
0.7	0.619	−0.014	0.007	0.668	−0.007	0.007	0.712	−0.014	0.005
1	0.616	−0.012	0.007	0.667	−0.007	0.008	0.714	−0.013	0.006
4	0.653	−0.008	0.008	0.678	−0.006	0.008	0.725	−0.009	0.007
7	0.669	−0.006	0.008	0.685	−0.005	0.008	0.748	−0.008	0.007
10	0.677	−0.006	0.008	0.689	−0.005	0.008	0.761	−0.007	0.007
100	0.698	−0.005	0.008	0.699	−0.005	0.008	0.787	−0.005	0.007
1000	0.699	−0.005	0.008	0.699	−0.005	0.008	0.762	−0.006	0.007
∞	0.699	−0.005	0.008	0.699	−0.005	0.008	0.763	−0.006	0.007

TABLE 2. Values of H_{r1}, H_{r2} and H_{r3} with boundaries of different conductivity

	$\gamma_b = \gamma_t = \gamma$			$\gamma_b = \gamma, \gamma_t = \infty$			$\gamma_b = \gamma, \gamma_t = 0$		
γ	H_{s1}	H_{s2}	H_{s3}	H_{s1}	H_{s2}	H_{s3}	H_{s1}	H_{s2}	H_{s3}
0	0.786	−0.001	0.002	0.865	0.026	0.043	0.786	−0.001	0.002
0.0001	0.786	0	−0.000	0.865	0.026	0.043	0.786	0	0
0.001	0.780	0	0.000	0.838	0.026	0.043	0.782	0	0
0.01	0.711	−0.004	0.004	0.821	0.025	0.044	0.713	−0.004	0.003
0.1	0.623	−0.006	0.011	0.802	0.026	0.045	0.650	−0.006	0.010
0.4	0.590	−0.001	0.022	0.760	0.027	0.048	0.686	−0.002	0.018
0.7	0.599	0.008	0.034	0.736	0.029	0.052	0.705	0.002	0.023
1	0.618	0.013	0.040	0.734	0.030	0.053	0.749	0.006	0.026
4	0.705	0.029	0.054	0.747	0.035	0.059	0.841	0.019	0.036
7	0.732	0.034	0.059	0.758	0.037	0.061	0.912	0.024	0.038
10	0.744	0.035	0.060	0.764	0.038	0.062	0.954	0.027	0.038
100	0.776	0.040	0.063	0.779	0.040	0.064	1.031	0.032	0.040
1000	0.779	0.040	0.064	0.779	0.040	0.064	0.948	0.030	0.042
∞	0.779	0.040	0.064	0.779	0.040	0.064	0.949	0.030	0.042

TABLE 3. Values of H_{s1}, H_{s2} and H_{s3} with boundaries of different conductivity

$\gamma_1 \leqslant 0.6$ for case III). $H_r = \max(H_r, H_s, H_h)$ for all $\gamma > \gamma_1$. γ_1 is found to decrease with decreasing P, and $\gamma_1 \rightarrow 0$ as $P \rightarrow 0$. The qualitative features of H_r, H_s and H_h (as well as R_c and α_c) are found to be symmetric with respect to γ_b and γ_t.

The stability of ϕ and θ with respect to arbitrary three-dimensional disturbances $\tilde{\phi}$ and $\tilde{\theta}$ is investigated in the same way as discussed in R83. The equations for the time-dependent disturbances are given by

$$\Delta_2(\nabla^4\tilde{\phi} - \tilde{\theta} - \sigma\nabla^2\tilde{\phi}) = P^{-1}\boldsymbol{\delta}\cdot[\boldsymbol{\delta}\tilde{\phi}\cdot\nabla(\boldsymbol{\delta}\phi) + \boldsymbol{\delta}\phi\cdot\nabla(\boldsymbol{\delta}\tilde{\phi})], \tag{15a}$$

$$(\nabla^2 - \sigma)\tilde{\theta} - R\Delta_2\tilde{\phi} = \boldsymbol{\delta}\tilde{\phi}\cdot\nabla\theta + \boldsymbol{\delta}\phi\cdot\nabla\tilde{\theta}, \tag{15b}$$

	$\gamma_b=\gamma_t=\gamma$			$\gamma_b=\gamma,\ \gamma_t=\infty$			$\gamma_b=\gamma,\ \gamma_t=0$		
γ	H_{h1}	H_{h2}	H_{h3}	H_{h1}	H_{h2}	H_{h3}	H_{h1}	H_{h2}	H_{h3}
0	1.143	0.032	0.050	0.956	0.031	0.045	1.143	0.032	0.050
0.0001	1.134	0.037	0.051	0.956	0.031	0.045	1.065	−0.087	0.002
0.001	1.135	0	0	0.939	0.031	0.046	1.138	0	0
0.01	1.039	−0.005	0.004	0.926	0.031	0.046	1.041	−0.005	0.004
0.1	0.895	−0.007	0.012	0.911	0.032	0.047	0.929	−0.007	0.011
0.4	0.806	0	0.023	0.875	0.034	0.051	0.900	−0.002	0.019
0.7	0.777	0.013	0.036	0.857	0.037	0.055	0.886	0.004	0.024
1	0.780	0.020	0.042	0.855	0.038	0.056	0.903	0.008	0.027
4	0.835	0.038	0.057	0.867	0.045	0.063	0.942	0.022	0.038
7	0.855	0.044	0.063	0.876	0.047	0.065	0.980	0.026	0.040
10	0.864	0.046	0.064	0.881	0.048	0.066	1.003	0.027	0.040
100	0.891	0.049	0.068	0.893	0.050	0.068	1.046	0.031	0.042
1000	0.893	0.050	0.068	0.893	0.050	0.068	1.003	0.031	0.044
∞	0.893	0.050	0.068	0.893	0.050	0.068	1.004	0.031	0.044

TABLE 4. Values of H_{h1}, H_{h2} and H_{h3} with boundaries of different conductivity

where we have introduced a growth rate σ by $\partial/\partial t=\sigma$. The stability equations are solved by the following expansions

$$\begin{pmatrix}\tilde{\phi}\\ \tilde{\theta}\\ \sigma\end{pmatrix}=\begin{pmatrix}\tilde{\phi}_1\\ \tilde{\theta}_1\\ \sigma_0\end{pmatrix}+\epsilon\begin{pmatrix}\tilde{\phi}_2\\ \tilde{\theta}_2\\ \sigma_1\end{pmatrix}+\epsilon^2\begin{pmatrix}\tilde{\phi}_3\\ \tilde{\theta}_3\\ \sigma_2\end{pmatrix}+\dots. \quad (16)$$

We restrict our attention to the most dangerous disturbances (where $R_0=R_c$ and $\alpha=\alpha_c$). Then the most critical disturbances are characterized by $\sigma_0=0$. Using the representation

$$\tilde{w}(x,y)=\sum_{n=-\infty}^{\infty}\tilde{c}_n\exp(\mathrm{i}\boldsymbol{k}_n\cdot\boldsymbol{r}) \quad (17)$$

for the horizontal dependence of the general three-dimensional disturbances, we consider (15) in orders ϵ^n $(n\geqslant 1)$. The possibility of a non-vanishing positive coefficient σ_n appears first at order ϵ^2, where the solvability condition (see the Appendix) yields the following system of equations:

$$\sigma_2\langle\theta_1^2\rangle\tilde{c}_n+c_n\sum_{m=-N}^{N}\tilde{T}_{nm}c_m^*\tilde{c}_m=0, \quad (18a)$$

where
$$\tilde{T}_{nm}=T_{nm}+T_{n,-m}. \quad (18b)$$

This system is of the same form as the one determined in R83. Following R83, it follows that a steady solution for $N>1$ is unstable if

$$\tilde{T}_{nm}>\tilde{T}_{nn}>0 \quad (m>n) \quad (19)$$

and that steady rolls $(N=1)$ are unstable if the steady squares $(N=2)$ are stable or *vice versa*. The condition (19) has been computed numerically for different integers N and various values of $\hat{\phi}_{mn}$ $(0\leqslant|\hat{\phi}_{mn}|\leqslant 1)$. In all cases of N and $\hat{\phi}_{mn}$ that have been investigated the condition (19) was found to be valid, with the exception of the

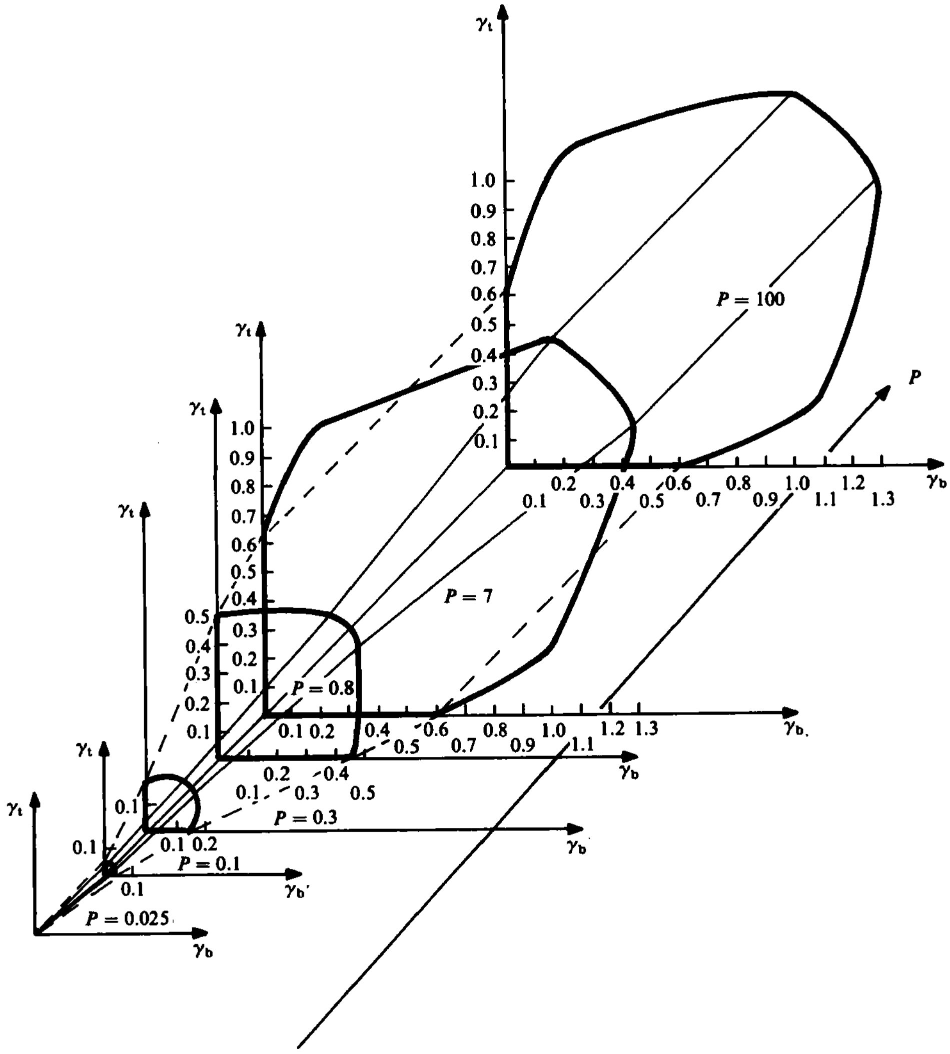

FIGURE 1. Region of stable square cells in the (γ_b, γ_t, P)-space coordinate system.

case $N = 2$, $\phi_{mn} = 0$ $(m \neq n)$. This latter case corresponds to squares. Hence all three-dimensional solutions for $N > 2$ are unstable. For squares it was found that (19) does not hold for those values of P, γ_b and γ_t that yield $H_s > H_r$. Numerical computations of the expression for σ_2 for disturbances that may or may not coincide with the basic vectors of the steady motions in the forms of squares and rolls yield a negative σ_2, provided that P, γ_b and γ_t are chosen such that $H_s > H_r$ and $H_r > H_s$ respectively. The general conclusion is that rolls and squares are the only possible stable solutions. Rolls are the only stable solutions in the (γ_b, γ_t, P)-space for which $H_r \geqslant H_s$. Squares are the only stable solutions in the (γ_b, γ_t, P)-space for which $H_s \geqslant H_r$.

In order to determine the stability boundary for rolls or squares in the

(γ_b, γ_t, P)-space coordinate system, the equation

$$\tilde{T}_{12} = \tilde{T}_{11} \quad (\text{equivalent to } H_s = H_r) \tag{20}$$

is solved numerically, and the results are shown in figure 1. Squares are the stable solutions in the semi-infinite three-dimensional region Ω which begins at the origin $\gamma_b = \gamma_t = P = 0$. Several cross-sectional areas of Ω ($P = 0.025, 0.1, 0.3, 0.8, 7, 100$) are shown in the figure. The area A of the cross-section of Ω with plane $P =$ constant is quite small in the range $0 \leqslant P \leqslant 0.1$. However, A increases rapidly with increasing P in the range $0.1 < P \leqslant 7$. For $P \geqslant 100$ the area A remains nearly unchanged as P increases. The stability boundary is also seen to be symmetric with respect to γ_b and γ_t.

3. Discussion

We investigated the problem of weakly nonlinear convection in a horizontal fluid layer of arbitrary P, γ_b and γ_t in the limit of very large thicknesses D_t and D_b of the upper and lower rigid surfaces respectively that bound the fluid layer. Using the method of Schlüter *et al.* (1965), we solved the nonlinear problem and determined the preferred mode of convection. The analysis led to the following conclusions. Square cells are the preferred form of convection in a semi-infinite three-dimensional region Ω in the (γ_b, γ_t, P)-space. Two-dimensional rolls are the preferred form of convection outside Ω. The region of stable squares is quite small for $P \leqslant 0.025$ and disappears as $P \rightarrow 0$ (consistent with the earlier result given by Riahi (1980) for $P = 0$ and $\gamma_b = \gamma_t \ll 1$). The region of stable squares is largest and nearly independent of P for $P \geqslant 7$. Also for large P ($P \geqslant 7$), the horizontal size of stable square cells can be comparable to the size of the layer depth, but the horizontal size of stable square cells is always much larger than the size of the layer depth for small P ($P \leqslant 0.1$). The region of stable squares is found to be most sensitive to P in the range $0.1 \leqslant P \leqslant 7$. The stable solution is found to transport the maximum amount of heat. The heat transported by convection and the critical values of R_c and α_c are found to be more sensitive to γ_b and γ_t in the midrange of these parameters. Qualitative features of Rayleigh–Bénard convection appear to be symmetric with respect to γ_b and γ_t. The only preferred flow pattern is that of either squares or rolls (but not both), and no hysteresis effect is found in the present problem. If γ_b or γ_t or both are sufficiently large, then the only stable flow pattern is that of two-dimensional rolls. It is also found that the qualitative results of the problem for asymmetric boundary conditions ($\gamma_b \neq \gamma_t$) can be quite different from those for symmetric boundary conditions ($\gamma_b = \gamma_t$). In particular, squares are unstable for the case of a strongly asymmetric boundary conditions where γ_b and γ_t are sufficiently different.

In the study of the transition from roll to square-cell solutions in the weakly nonlinear convection in a layer with symmetric boundary conditions ($\gamma_b = \gamma_t \equiv \gamma$) presented in JP, a perturbation technique, a finite-difference method and an iteration technique were employed to calculate R_c, α_c and the critical values of γ_c (at which transition from rolls to squares takes place) as functions of P and D ($D \equiv D_t = D_b$). The linear result for the values of R_c and α_c presented in JP for $D = 1$ agrees well with the corresponding result of the present study (columns 2 and 3 in table 1) for $D \gg 1$. Another result in JP is about the effects of D on γ_c, which demonstrates that $\gamma_c = O(D)$ for small D, while γ_c is independent of D for large D. This result is in agreement with the earlier result derived by Busse & Riahi (1980), which indicated that various flow features are independent of D as long as D is considerably larger than one. Figure 3 in JP shows variations of γ_c with respect to P for both cases $D = 1$ and $D \gg 1$. γ_c becomes independent of P for $P > 10$, and approaches one for large P. The results for γ_c ($D \gg 1$) given in JP are in qualitative agreement with the corresponding results of the present study for the case $\gamma_b = \gamma_t$. There do not appear to be other similarities between the results of the present study and that discussed in JP. The work presented in JP is mainly for γ_c and its variations with respect to P and D for a fluid layer with symmetric boundary conditions, while the present paper studies both cases of symmetric and asymmetric boundary conditions for arbitrary values of P, γ_b and γ_t, and presents results for the asymmetric boundary conditions, which can sharply differ qualitatively from the corresponding results for the symmetric boundary conditions. In addition, the present study yields results for various flow features for the complete domain of small-amplitude convection with arbitrary conducting boundaries, which can be of particular interest to experimentalists, and it is hoped that it will stimulate experimental studies on the subject.

Appendix

To order ϵ, the equations (2) and the boundary conditions (3) become

$$\Delta_2(\nabla^4\phi_1-\theta_1) = 0, \tag{A 1a}$$

$$\nabla^2\theta_1 - R_0\Delta_2\phi_1 = 0, \tag{A 1b}$$

$$\phi_1 = \frac{\partial\phi_1}{\partial z} = \left(\frac{\partial}{\partial z} \pm \alpha\gamma_\pm\right)\theta_1 = 0 \quad \text{at } z = \pm\tfrac{1}{2}, \tag{A 1c}$$

where $\gamma_+ \equiv \gamma_t$ and $\gamma_- \equiv \gamma_b$ (see R83 for the derivation of the thermal boundary conditions). Equations (A 1a, b) yield

$$\begin{pmatrix}\theta_1\\ \phi_1\end{pmatrix} = \begin{pmatrix} g(z)\\ f(z)\end{pmatrix} w(x,y), \tag{A 2}$$

where

$$\left.\begin{aligned} f(z) &= \sum_{i=1}^{6} d_i \exp(r_i z) \quad \langle f^2\rangle = 1,\\ g(z) &= \sum_{i=1}^{6} (r_i-\alpha^2)^2 d_i \exp(r_i z),\\ r_1 = -r_4 &= [\alpha^2-(R_0\alpha^2)^{\frac{1}{3}}]^{\frac{1}{2}},\\ r_2 = -r_5 &= [\alpha^2+(R_0\alpha^2)^{\frac{1}{3}}\exp(-\tfrac{1}{3}i\pi)]^{\frac{1}{2}},\\ r_3 = -r_6 &= [\alpha^2+(R_0\alpha^2)^{\frac{1}{3}}\exp(\tfrac{1}{3}i\pi)]^{\frac{1}{2}}. \end{aligned}\right\} \tag{A 3}$$

When (A 2) and the expressions for $f(z)$ and $g(z)$ given in (A 3) are used in (A 1) they yield a system of six linear non-homogeneous algebraic equations for the coefficients d_i ($i = 1, \ldots, 6$). This system of equations together with the normalization condition for $f(z)$ given in (A 3) lead to an implicit functional dependence of R_0 with respect to α, γ_b and γ_t.

To order ϵ^2, the equations (2) and the boundary conditions (3) become

$$\Delta_2(\nabla^4\phi_2-\theta_2) = P^{-1}[\boldsymbol{\delta}\cdot(\boldsymbol{\delta}\phi_1\cdot\nabla\boldsymbol{\delta}\phi_1)], \tag{A 4a}$$

$$\nabla^2\theta_2 - R_0\Delta_2\phi_2 - R_1\Delta_2\phi_1 = \boldsymbol{\delta}\phi_1\cdot\nabla\theta_1, \tag{A 4b}$$

$$\phi_2 = \frac{\partial\phi_2}{\partial z} = \frac{\partial\theta_2}{\partial z} \pm \gamma_\pm\,\theta_{2s} = 0 \quad \text{at } z = \pm\tfrac{1}{2}, \tag{A 4c}$$

where θ_{2s} (defined in R83) has the same form as θ_2, provided that the horizontal dependence of θ_2 is multiplied by $[2(\alpha^2+\boldsymbol{K}_l\cdot\boldsymbol{K}_p)]^{\frac{1}{2}}$. The reader is referred to R83 for discussion on the boundary conditions for θ. Multiplying (A 4*a*) by ϕ_1, (A 4*b*) by $R_0^{-1}\theta_1$, adding, averaging over the whole layer and using the procedure used by Schlüter *et al.* (1965) yields $R_1 = 0$. The expressions for the solutions θ_2 and ϕ_2 that satisfy (A 4) are quite lengthy and will not be given here. The complete expressions for these quantities as well as the lengthy expressions for some other quantities are given in an internal report which can be made available to the reader upon request.

To order ϵ^3, (2) become

$$\Delta_2(\nabla^4\phi_3-\theta_3) = p^{-1}[\boldsymbol{\delta}\cdot(\boldsymbol{\delta}\phi_1\cdot\nabla\boldsymbol{\delta}\phi_2+\boldsymbol{\delta}\phi_2\cdot\nabla\boldsymbol{\delta}\phi_1)], \tag{A 5a}$$

$$\nabla^2\theta_3-R_0\Delta_2\phi_3-R_2\Delta_2\phi_1 = \boldsymbol{\delta}\phi_1\cdot\nabla\theta_2+\boldsymbol{\delta}\phi_2\cdot\nabla\theta_1. \tag{A 5b}$$

The solvability condition for (A 5) requires us to define the following special solutions θ_{1n} and ϕ_{1n} of (A 1):

$$\begin{pmatrix}\theta_{1n}\\ \phi_{1n}\end{pmatrix} = \begin{pmatrix}g(z)\\ f(z)\end{pmatrix} w_n. \tag{A 6}$$

Multiplying (A 5*a*) by ϕ_{1n}^*, (A 5*b*) by $R_0^{-1}\theta_{1n}^*$, adding and averaging over the whole layer yields

$$-R_2\langle\theta_{1n}^*\Delta_2\phi_1\rangle = \langle\theta_{1n}^*(\boldsymbol{\delta}\phi_1\cdot\nabla\theta_2)\rangle+p^{-1}R_0\langle\phi_{1n}^*\boldsymbol{\delta}\cdot(\boldsymbol{\delta}\phi_1\cdot\nabla\boldsymbol{\delta}\phi_2+\boldsymbol{\delta}\phi_2\cdot\nabla\boldsymbol{\delta}\phi_1)\rangle. \tag{A 7}$$

The right-hand side in (A 7) contains average products of the form $\langle w_n^* w_m w_l w_p\rangle$, which differ from zero only if

$$-\boldsymbol{K}_n+\boldsymbol{K}_m+\boldsymbol{K}_l+\boldsymbol{K}_p = 0. \tag{A 8}$$

Following R83 and using (A 8), (A 7) can be simplified to the form given in (9).

To order ϵ^2, (15) become

$$\Delta_2(\nabla^4\tilde{\phi}_3-\tilde{\theta}_3-\sigma_2\nabla^2\tilde{\phi}_1) = p^{-1}\boldsymbol{\delta}\cdot[\boldsymbol{\delta}\tilde{\phi}_1\cdot\nabla\boldsymbol{\delta}\phi_2+\boldsymbol{\delta}\phi_1\cdot\nabla\boldsymbol{\delta}\tilde{\phi}_2+\boldsymbol{\delta}\tilde{\phi}_2\cdot\nabla\boldsymbol{\delta}\phi_1+\boldsymbol{\delta}\phi_2\cdot\nabla\boldsymbol{\delta}\tilde{\phi}_1], \tag{A 9a}$$

$$\nabla^2\tilde{\theta}_3-\sigma_2\tilde{\theta}_1-R_0\Delta_2\tilde{\phi}_3-R_2\Delta_2\tilde{\phi}_1 = \boldsymbol{\delta}\tilde{\phi}_1\cdot\nabla\theta_2+\boldsymbol{\delta}\phi_1\cdot\nabla\tilde{\theta}_2+\boldsymbol{\delta}\tilde{\phi}_2\cdot\nabla\theta_1+\boldsymbol{\delta}\phi_2\cdot\nabla\tilde{\theta}_1. \tag{A 9b}$$

Here the solutions $\tilde{\theta}_1$ and $\tilde{\phi}_1$ have the same form as the corresponding steady solutions θ_1 and ϕ_1, provided the horizontal dependence of the steady solutions is replaced by the expression (17). Likewise, the solutions $\tilde{\theta}_2$ and $\tilde{\phi}_2$ have the same form as the corresponding steady solutions θ_2 and ϕ_2, provided the coefficients $c_l c_p$ in the horizontal-dependent terms in the expressions for these solutions are replaced by $2\tilde{c}_l c_p$ ($l = -\infty, \ldots, -1, 1, \ldots, \infty$ and $p = -N, \ldots, -1, 1, \ldots, N$), and the horizontal-independent terms in the expressions for the steady solutions are multiplied by the expression $\Sigma_{m=-N}^{N} 2\tilde{C}_m C_m^*$. Multiplying (A 9*a*) by ϕ_{1n}^*, (A 9*b*) by $R_0^{-1}\theta_{1n}^*$, adding, averaging over the whole layer, using (A 8) and following the same procedure as in R83 yields (18).

REFERENCES

Busse, F. H. & Riahi, N. 1980 Nonlinear convection in a layer with nearly insulating boundaries. *J. Fluid Mech.* **96**, 243–256.

Jenkins, D. R. & Proctor, M. R. E. 1984 The transition from roll to square-cell solutions in Rayleigh–Bénard convection. *J. Fluid Mech.* **139**, 461–471.

RIAHI, N. 1980 On convection with nearly insulating boundaries in a low Prandtl number fluid. *Z. angew. Math. Phys.* **31**, 261–266.

RIAHI, N. 1983 Nonlinear convection in a porous layer with finite conducting boundaries. *J. Fluid Mech.* **129**, 153–171.

SCHLÜTER, A., LORTZ, D. & BUSSE, F. H. 1965 On the stability of finite amplitude convection. *J. Fluid Mech.* **23**, 129–144.